Angiogenesis 4: 263–268, 2001.

Original article

Statin-AE: A novel angiostatin–endostatin fusion protein with enhanced antiangiogenic and antitumor activity

Frank A. Scappaticci[1], Anthony Contreras[2], Richard Smith[2], Loic Bonhoure[2], Bert Lum[3], Yihai Cao[4], Edgar G. Engleman[1,3] & Garry P. Nolan[2]

Departments of [1]Pathology, [2]Molecular Pharmacology, [3]Microbiology and Immunology Medicine, Stanford University Medical Center, Stanford, California, USA; [4]Laboratory of Angiogenesis Research, Microbiology, Tumor Biology Center, Karolinska Institute, Stockholm, Sweden

Received 19 December 2000; accepted in revised form 6 August 2001

Key words: angiogenesis inhibitor, endothelial cells, gene therapy, melanoma, retrovirus

Abstract

The combination of angiostatin and endostatin has been shown to have synergistic antiangiogenic and antitumor effects when the genes for these proteins are delivered to tumor cells by retroviral gene transfer. Here we report the construction of a murine angiostatin–endostatin fusion gene (Statin-AE) which shows enhanced antiangiogenic activity on human umbilical vein endothelial cell (HUVEC) tube formation *in vitro* compared with angiostatin or endostatin alone. Similarly, the fusion gene demonstrates antiangiogenic effects *in vivo* and antitumor activity in a B16F10 melanoma model when co-delivered by retroviral packaging cell inoculation in mice. The fusion gene demonstrates significantly greater inhibition of tumor growth compared with angiostatin, endostatin or the combination of genes.

Introduction

Angiostatin and endostatin are two potent antiangiogenic proteins that have individually demonstrated antitumor activity in multiple murine tumor models both in prevention and treatment of established tumors [1–9]. These proteins appear to induce apoptosis in endothelial cells but do not have cytotoxic effects on other cell types including tumor cells [1, 2, 10]. There have been several reports which suggest that a combination of antiangiogenic factors may demonstrate additive or even synergistic inhibition of angiogenesis and tumor growth. In particular, the combination of angiostatin and endostatin has been shown to have potent inhibitory activity on the growth of spontaneous tumors in a rat pancreatic islet tumor model and may be synergistic in the treatment of ovarian cancer in a nude mouse model [11, 12]. We have previously shown that the combination of angiostatin and endostatin delivered as single molecules by retroviral gene transfer has synergistic inhibitory activity on the growth of B16F10 melanoma tumors compared with angiostatin or endostatin alone [13]. Similarly, in a murine L1210 leukemia model, expression of both these genes resulted in failure of leukemic tumor growth in 40% of mice [13].

Based on these findings, we report the construction of a novel angiostatin–endostatin fusion gene that demonstrates potent antiangiogenic activity *in vitro* and antitumor activity *in vivo*. Compared with angiostatin or endostatin alone, the fusion protein demonstrates greater than additive activity on inhibition of HUVEC tube formation *in vitro* and potent antitumor effects in a B16F10 melanoma model *in vivo*.

Materials and methods

Construction of retroviral vectors

The Lazarus (LZRS)-based Moloney murine leukemia viral (MMuLV) vectors were constructed by cloning the cDNA fragments of mouse angiostatin [4] or mouse endostatin [9] (these were generous gifts from Y. Cao and T. Boehm, respectively) into the Bam H1 or Bgl II/Xho I sites, respectively, upstream of the internal ribosomal entry site (IRES) and green fluorescent protein (GFP) sequences of the LZRS IRES–GFP plasmid [14]. The 5′ signal sequences that allow for secretion of angiostatin and endostatin were derived from plasminogen or collagen XVIII, respectively. The

Correspondence to: Garry P. Nolan, PhD, Associate Professor, Department of Molecular Pharmacology, Stanford University School of Medicine, 269 Campus Drive, CCSR 3220, Stanford, CA 94305-5174, USA. Tel: +1-650-732-7875; Fax: +1-650-725-2952; E-mail: gnolan@cmgm.stanford.edu

angiostatin–endostatin fusion gene was created by inserting an Nde I-Nhe I adaptor sequence (5′-catatggctagccatatg-3′) at the 3′ end of angiostatin and 5′ of endostatin. The fusion gene was cloned into the EcoR1 and XhoI sites of the LZRS IRES–GFP plasmid. When transfected into Phoenix amphotropic retroviral packaging cells, these vectors produce replication defective virus with a titer of approximately 1.0×10^6 as determined by GFP expression of infected NIH 3T3 fibroblasts (data not shown).

Transfection/transduction of tumor cells/FACS

Calcium phosphate transfection of Phoenix cells has been described elsewhere [15]. Selection of GFP expressing Phoenix cell transfectants or infected B16F10 melanoma cells was by flow cytometry using a FACStar Plus cell sorter (Becton Dickinson) set at 488 nm excitation wavelength. Gates were set to sort the highest 25% of fluorescent cells and the cells were collected in PBS. Growth of B16F10 melanoma cells was determined by standard MTT assay (580 nm absorbance).

Matrigel assays

Growth factor reduced matrigel was obtained from Becton Dickinson. The matrigel was allowed to solidify for 1 h in serum free media (EBM from Clonetics) in the wells of six well culture plates. HUVECs were also obtained from Clonetics. The endothelial cells (2×10^5 cells/well) were plated on matrigel with 2.5 volumes of filtered viral supernatants harvested from B16F10 melanoma cells expressing angiostatin, endostatin, or Statin-AE. Approximately 3–24 h later, the cells were analyzed under a light microscope for tube formation [16]. Dose–response effects of the Statin-AE protein were assessed using dilutions of the supernatants in media and counting the number of endothelial cell tubes.

Microvessel density studies

C57BL/6 mice were inoculated subcutaneously with B16F10 melanoma tumors (1.0×10^5 cells) expressing GFP alone or Statin-AE–IRES–GFP. After 2 weeks of tumor growth, tumors were resected and fixed in 10% paraformaldehyde. Formalin sections were blocked followed by antigen retrieval using citra antigen retrieval (Biogenex). The sections were then stained with biotinylated rat anti-PECAM-1 monoclonal antibody (clone MEC 13.3 – Pharmingen) at 1:50 dilution. This was followed by incubation with avidin-HRP (Biogenex) and DAB substrate. Microvessel density was scored as an average of five random fields (20×) [17].

Mouse tumorigenicity studies

For B16F10 melanoma studies, C57BL/6 female mice (6–8 weeks old, Jackson Labs) were injected subcutaneously in the left flank with 200 μl volume of 1.0×10^5 melanoma cells + 1.0×10^5 packaging cells. The latter had been selected for the 25% highest GFP expression by flow cytometry. Tumors were measured with calipers in three dimensions approximately every 3–4 days and recorded as volume (cm^3). Tumor growth rates *in vitro* and *in vivo* were compared using exponential regression analysis [18]. Non-overlapping 95% confidence intervals of the regression parameter (K) were statistically significant at $P \leq 0.05$.

Results and discussion

The retroviral vector containing the angiostatin–endostatin fusion gene (shown in Figure 1a) was constructed with angiostatin in the 5′ location and fused to endostatin via an HA tag sequence. Transfection of retroviral vectors into Phoenix amphotropic packaging cells yielded infectious virus with a titer of 1×10^6 as determined on NIH 3T3 cells. Infected B16F10 mela-

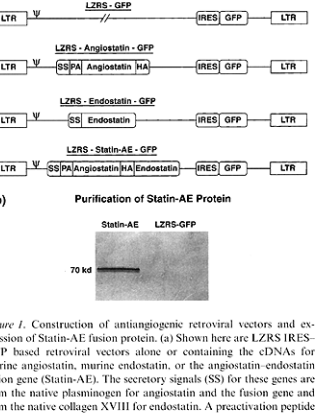

Figure 1. Construction of antiangiogenic retroviral vectors and expression of Statin-AE fusion protein. (a) Shown here are LZRS IRES–GFP based retroviral vectors alone or containing the cDNAs for murine angiostatin, murine endostatin, or the angiostatin–endostatin fusion gene (Statin-AE). The secretory signals (SS) for these genes are from the native plasminogen for angiostatin and the fusion gene and from the native collagen XVIII for endostatin. A preactivation peptide sequence (PA) is located 3′ to the secretory signal and immediately preceding the angiostatin gene. A short HA tag sequence was added to the 3′ end of the angiostatin gene and serves as a linker between angiostatin and endostatin in the fusion construct. (b) Secretion of Statin-AE from B16F10 melanoma cells. Fusion protein in pooled supernatants from 1.0×10^7 B16F10 melanoma cells was purified using lysine-sepharose chromatography followed by elution with 0.2 mM e-aminocaproic acid. After dialysis in PBS, aliquots (1 μg) were subjected to SDS-PAGE followed by coomassie blue staining. Confirmation of the angiostatin–endostatin fusion protein was achieved after transfer of the protein to PVDF membrane followed by Edman degradation using an ABI Procise.

noma cells for *in vitro* studies and infected Phoenix cells for *in vivo* studies were enriched by sorting for expression of the GFP comarker protein by flow cytometry (data not shown). Expression of the fusion gene was determined by rt-PCR using primers directed against angiostatin or endostatin (Figure 2). Expression of GFP was also determined by rt-PCR after sorting of the highest 25% GFP-expressing Phoenix packaging cells. Expression of the transgene-IRES GFP transcript was very similar in Phoenix cells as compared with standardized actin controls. Similarly, expression of angiostatin was seen only in cells expressing angiostatin or the fusion gene. Endostatin expression was also observed in cells expressing endostatin or the fusion gene. Secretion of Statin-AE from infected cells was shown by SDS-PAGE after lysine sepharose purification of the protein in supernatant from B16F10 melanoma cells (Figure 1b). A protein of molecular weight 70 kd was seen which in some preparations from other tumor cell types migrates at 55 kd and may be related to differences in glycosylation. The protein could be purified to >90% purity and was not seen in similarly prepared samples from control LZRS–GFP supernatant. Approximately 50 nM of protein was estimated to be present in the supernatants of B16F10 cells. N-terminal sequencing of the protein revealed a 17 amino acid sequence (DLLDDY-VNTQGASLLSL) which confirmed the N-terminus of the angiostatin–endostatin fusion protein. Thus, we felt confident that the fusion protein produced from these cells represents a bona fide fusion of appropriate length. Previously, we showed secretion of angiostatin and endostatin from B16F10 cells and other cell types [13]. Statin-AE showed little reactivity on Western blots after probing with anti-HA monoclonal antibody. This

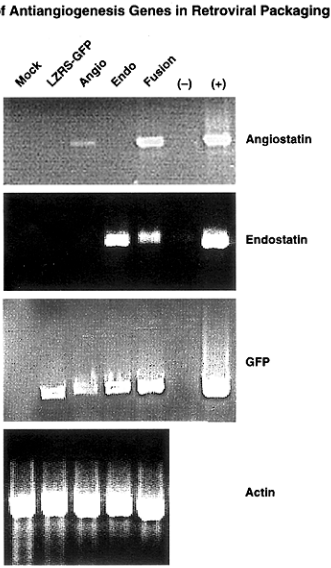

Figure 2. Expression of Statin-AE fusion gene in Phoenix retroviral packaging cells. RNA preparation and rt-PCR of GFP, angiostatin, and endostatin were performed using a Qiagen Rneasy Mini kit and OneStep kit. B actin primers and amplification protocol were obtained from Clontech. The primers used for angiostatin amplification were 5′-AGAATGTAAGACCGGCATCG-3′ and 5′-CCTCTGGTGGAACTGA-GGAA-3′. For endostatin amplification the sequences were 5′-ATTCGTATCTCGAGCATACTCATCAGGACTTTCAG-3′ and 5′-GCCTAA-GAATTCCTATTTGGAGAAAGAGGTCAT-3′. The primers used for GFP amplification were 5′-CAAGGGCGAGGAGCTGTT-3′ and 5′-CTTGTACAGCTCGTCCATGC-3′. Controls labeled (–) were LZRS plasmids containing lacZ instead of GFP which underwent PCR amplification with each set of primers. The positive control (+) for angiostatin was pRc/CMV-angiostatin, for endostatin was LZRS-endostatin, and for GFP was LZRS–GFP.

suggests a loss of immunogenic epitopes when angiostatin and endostatin are fused (data not shown).

To determine antiangiogenic effects of the secreted Statin-AE fusion protein, we tested Statin-AE in matrigel assays to assess HUVEC differentiation *in vitro*. As seen in Figure 3a, a dose–response relationship exists with Statin-AE containing supernatants from B16F10 cells in that a marked tubular inhibitory effect was seen at 1× and 2/3× but was lost at 1/3 and 1/6 dilutions. At the higher concentrations of the fusion protein, the HUVECs appeared clustered without evidence of tube formation. There was no difference in the inhibition of tube formation among the mock, LZRS–GFP, angiostatin, or endostatin treated groups (Figure 3b). However, fusion 1× (undiluted) significantly inhibited tube formation compared with controls ($P \leq 0.05$) and was similar to the angiostatin/endostatin combination. Purified Statin-AE similarly inhibited tube formation

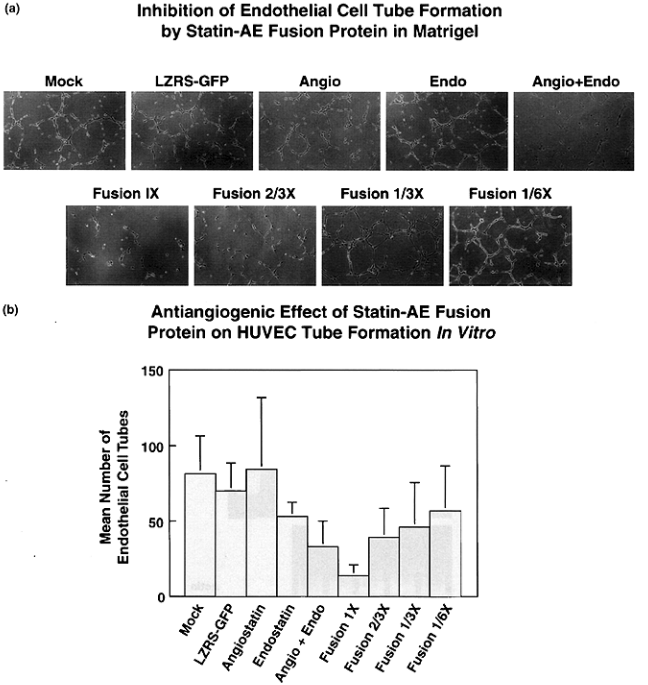

Figure 3. Antiangiogenic effect of Statin-AE on HUVEC tube formation in matrigel. (a) Dose–response effect of Statin-AE protein from B16F10 melanoma cell supernatants on HUVEC tube formation as seen under low power view. (b) Quantitation of tube formation of various doses of Statin-AE. B16F10 supernatants containing Statin-AE were diluted in DMEM conditioned media at 1:6, 1:3, 2:3, or no dilution (1×). Endothelial cell tubes were counted at 3 h after plating and were scored as the average of five high powered fields (similar results were seen in two other experiments both at 3 and 24 h). A Mann–Whitney test showed statistical significance comparing fusion 1× with 1:3 and 1:6 dilutions as well as all other groups ($P \leq 0.05$) except for angiostatin + endostatin combination ($P = 0.19$) and 2:3 dilution ($P = 0.11$).

compared with unpurified protein in cell supernatants. However, there was variability in its activity in different batches and may require stringent conditions or other cofactors for stability (data not shown).

To investigate antiangiogenic effects of Statin-AE *in vivo*, B16F10 melanoma cells were transduced with LZRS–GFP or LZRS–Statin-AE–GFP, sorted for high GFP expression, and injected into mice. After 2 weeks of growth, the tumors were resected, formalin-fixed, and stained with anti-PECAM-1 antibody to determine microvessel density. Figure 4 shows a higher vessel density for the LZRS–GFP group compared with Statin-AE (>fourfold, $P = 0.008$, Mann–Whitney *U*-test). This suggests that Statin-AE expression and subsequent secretion inhibited new blood vessel growth in a paracrine fashion. Such activity might play a role in the inhibition of tumor growth.

We chose a retroviral packaging cell system as a relevant clinical model to investigate gene therapy with antiangiogenic factors to prevent or treat established tumors. Although Statin-AE demonstrated antiangiogenic activity *in vitro* and *in vivo*, there was no inhibitory effect on tumor cells grown *in vitro*. This was shown after stable infection of B16F10 melanoma cells with Statin-AE containing retrovirus, selection of GFP positive cells by flow cytometry, and assessment of cell growth *in vitro* by MTT assay. As shown in Figure 5a there was a slight but statistically significant growth advantage for cells expressing Statin-AE compared with mock, GFP alone, angiostatin, endostatin, or the combination of angiostatin and endostatin. The growth of B16F10 melanoma tumors was slowed *in vivo*, however, when retroviral packaging cells were delivered concomitantly with melanoma cells subcutaneously on the backs of C57BL/6 mice. As shown in Figure 5b, packaging cells expressing the fusion gene delayed tumor growth significantly when compared with the group receiving B16F10 cells alone or groups co-injected with packaging cells expressing LZRS–GFP, angiostatin, endostatin, or an equal mixture of cells expressing angiostatin and endostatin ($P \leq 0.05$). The effect may be through angiogenic inhibition by Statin-AE *in vivo*. Delivery of packaging cells expressing angiostatin, endostatin, or the combination slowed tumor growth compared with melanoma cells injected alone ($P \leq$

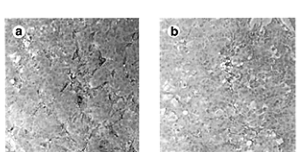

Figure 4. Inhibition of angiogenesis *in vivo* by Statin-AE. B16F10 melanoma tumors that were transduced by LZRS–GFP (a) or LZRS–Statin-AE–GFP (b) were grown in mice for 2 weeks and then analyzed for microvessel density. Shown here are formalin-fixed sections of tumors that have been stained with anti-PECAM-1 antibody. The vessels are shown in brown and microvessel density determination was performed on five random fields in hot spots and represented as vessels per high powered field.

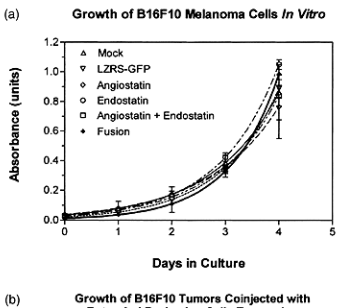

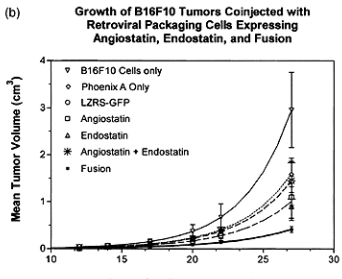

Figure 5. Statin-AE inhibits B16F10 melanoma tumor growth *in vivo* but does not directly inhibit tumor cell growth *in vitro*. (a) Melanoma cells that had been transduced with angiostatin, endostatin, or the Statin-AE fusion gene were assayed for growth *in vitro* using a standard MTT assay. Cells were plated at 2×10^3 per well and cell viability was assessed daily for 4 days. Data points were obtained from an average of five wells and were subjected to exponential curve fit. Exponential regression analysis showed a statistically significant growth advantage for the fusion group compared with the others ($P \leq 0.05$). There were no statistically significant differences between the other groups ($P > 0.05$). (b) To assess tumor growth in the presence of angiogenesis inhibitors, mice were injected with melanoma cells alone or in combination with Phoenix cells (that had been transfected with each of the various angiogenic inhibitors or controls). Shown here are the curve fitted plots for each group using an average of 10 animals per group at 3 day intervals. Exponential regression analysis through day 22 revealed significant differences when comparing the fusion group with B16F10 cells alone or Phoenix cells expressing LZRS–GFP, angiostatin, endostatin, or the combination ($P \leq 0.05$).

0.05). This may be related to an inflammatory or immune response to the xenogeneic packaging cell [19, 20]. The effect of the packaging cell on tumor growth inhibition was similar to that of cells expressing angiostatin or endostatin. It may be that angiostatin and endostatin have very little activity *in vivo* in this particular model or, alternatively, the effect of the packaging cell has masked this activity.

The mechanism of the antiangiogenic effect of Statin-AE *in vitro* and *in vivo* remains to be determined. Induction of apoptosis in endothelial cells is one possibility since the components of Statin-AE, angiostatin and endostatin, may be inducing apoptosis [10, 21]. It is possible that the induction of this process may be more potent than with either angiostatin or endostatin alone. This could be related to a binding avidity due to the combined affinities of the fused components of Statin-AE for two receptors on endothelial cells. Another explanation is that the conformation of the fusion protein has been modified leading to increased affinity for the receptor of either angiostatin or endostatin. Similarly, there may be an alteration of the stability, activity, or localization of Statin-AE *in vivo* which is conferred by one part of the fusion protein. Alternatively, the antiangiogenic effect may be related to displacement of angiogenic factors from the surface of endothelial cells through binding of heparan sulfate or integrins such as $\alpha_v\beta_3$ [22]. Finally, there may exist another receptor that is not related to the binding of angiostatin or endostatin alone, although this is least likely. It will be critical to determine if delivery of the protein directly into animals can induce regression of established tumors to a greater extent than angiostatin, endostatin, or the combination. The purification scheme we have implemented here for the angiostatin–endostatin fusion protein should, if successful in future studies, provide a reliable reagent for blocking angiogenesis *in vivo*. If so, further work may prove the reagent useful clinically in the treatment of cancer.

Acknowledgements

We wish to acknowledge the Lymphoma Research Foundation, Pfizer Fellowship, and the Janssen-ECOG Young Investigator grants for support of this work to FAS. This work was also supported in part by the NIH KO8 (CA79695-01A1) to FAS and NIH 1 R01 (AR/AI44565) to GPN.

References

1. O'Reilly MS, Holmgren L, Shing Y et al. Angiostatin: A novel angiogenesis inhibitor that mediates the suppression of metastases by a Lewis lung carcinoma. Cell 1994; 79(2): 315–28.
2. O'Reilly MS, Boehm T, Shing Y et al. Endostatin: An endogenous inhibitor of angiogenesis and tumor growth. Cell 1997; 88(2): 277–85.
3. Griscelli F, Li H, Bennaceur-Griscelli A et al. Angiostatin gene transfer: Inhibition of tumor growth *in vivo* by blockage of endothelial cell proliferation associated with a mitosis arrest. Proc Natl Acad Sci USA 1998; 95(11): 6367–72.
4. Tanaka T, Cao Y, Folkman J, Fine HA. Viral vector-targeted antiangiogenic gene therapy utilizing an angiostatin complementary DNA. Cancer Res 1998; 58(15): 3362–9.
5. Cao Y, O'Reilly MS, Marshall B et al. Expression of angiostatin cDNA in a murine fibrosarcoma suppresses primary tumor growth and produces long-term dormancy of metastases. J Clin Invest 1998; 101(5): 1055–63.
6. Ambs S, Dennis S, Fairman J et al. Inhibition of tumor growth correlates with the expression level of a human angiostatin transgene in transfected B16F10 melanoma cells. Cancer Res 1999; 59(22): 5773–7.
7. O'Reilly MS, Holmgren L, Chen C, Folkman J. Angiostatin induces and sustains dormancy of human primary tumors in mice. Nat Med 1996; 2(6): 689–92.
8. Dhanabal M, Ramchandran R, Volk R et al. Endostatin: Yeast production, mutants, and antitumor effect in renal cell carcinoma. Cancer Res 1999; 59(1): 189–97.
9. Boehm T, Folkman J, Browder T, O'Reilly MS. Antiangiogenic therapy of experimental cancer does not induce acquired drug resistance. Nature 1997; 390(6658): 404–7.
10. Dhanabal M, Ramchandran R, Waterman MJ et al. Endostatin induces endothelial cell apoptosis. J Biol Chem 1999; 274(17): 11721–6.
11. Bergers G, Javaherian K, Lo KM et al. Effects of angiogenesis inhibitors on multistage carcinogenesis in mice. Science 1999; 284(5415): 808–12.
12. Yokoyama Y, Dhanabal M, Griffioen AW et al. Synergy between angiostatin and endostatin: Inhibition of ovarian cancer growth. Cancer Res 2000; 60(8): 2190–6.
13. Scappaticci FA, Smith R, Pathak A et al. Combination angiostatin and endostatin gene transfer induces synergistic antiangiogenic activity *in vitro* and antitumor efficacy in leukemia and solid tumors in mice. Mol Ther 2001; 3(2): 186–96.
14. Kinsella TM, Nolan GP. Episomal vectors rapidly and stably produce high-titer recombinant retrovirus. Hum Gene Ther 1996; 7(12): 1405–13.
15. Kinoshita S, Chen BK, Kaneshima H, Nolan GP. Host control of HIV-1 parasitism in T cells by the nuclear factor of activated T cells. Cell 1998; 95(5): 595–604.
16. Riccioni T, Cirielli C, Wang X et al. Adenovirus-mediated wild-type p53 overexpression inhibits endothelial cell differentiation *in vitro* and angiogenesis *in vivo*. Gene Ther 1998; 5(6): 747–54.
17. Perez-Atayde AR, Sallan SE, Tedrow U et al. Spectrum of tumor angiogenesis in the bone marrow of children with acute lymphoblastic leukemia. Am J Pathol 1997; 150(3): 815–21.
18. Schwartz MA. Biomathematical approach to clinical tumor growth. Cancer 1961; 14(6): 1272–94.
19. Ram Z, Culver KW, Walbridge S et al. *In situ* retroviral-mediated gene transfer for the treatment of brain tumors in rats. Cancer Res 1993; 53(1): 83–8.
20. Ram Z, Culver KW, Oshiro EM et al. Therapy of malignant brain tumors by intratumoral implantation of retroviral vector-producing cells. Nat Med 1997; 3(12): 1354–61.
21. Dixelius J, Larsson H, Sasaki T et al. Endostatin-induced tyrosine kinase signaling through the Shb adaptor protein regulates endothelial cell apoptosis. Blood 2000; 95(11): 3403–11.
22. Sasaki T, Larsson H, Kreuger J et al. Structural basis and potential role of heparin/heparan sulfate binding to the angiogenesis inhibitor endostatin. EMBO J 1999; 18(22): 6240–8.